STEM CELLS

TISSUE-SPECIFIC STEM CELLS

p107 Is a Crucial Regulator for Determining the Adipocyte Lineage Fate Choices of Stem Cells

MARTINA DE SOUSA,[a] DEANNA P. PORRAS,[a,b] CHRISTOPHER G. R. PERRY,[b] PATRICK SEALE,[c] ANTHONY SCIMÈ[a,b]

Key Words. Beige or brite adipocytes • Brown adipocytes • Lineage commitment • PRDM16 • Mesenchymal stem cells • p107

[a]Stem Cell Research Group, Faculty of Health, York University, Toronto, Ontario, Canada; [b]Molecular, Cellular and Integrative Physiology, Faculty of Health, York University, Toronto, Ontario, Canada; [c]Cell and Developmental Biology, Institute for Diabetes, Obesity and Metabolism, University of Pennsylvania School of Medicine, Philadelphia, Pennsylvania, USA

Correspondence: Anthony Scimè, Ph.D., Stem Cell Research Group, Faculty of Health, York University, Toronto, Ontario, Canada M3J 1P3. Telephone: 1-416-736-2100, ext. 33559; Fax: 1-416-736-5774; e-mail: ascime@yorku.ca

Received June 4, 2013; accepted for publication November 20, 2013; first published online in STEM CELLS *EXPRESS* January 21, 2014.

1066-5099/2014/$30.00/0

http://dx.doi.org/10.1002/stem.1637

ABSTRACT

Thermogenic (beige and brown) adipocytes protect animals against obesity and metabolic disease. However, little is known about the mechanisms that commit stem cells toward different adipocyte lineages. We show here that p107 is a master regulator of adipocyte lineage fates, its suppression required for commitment of stem cells to the brown-type fate. p107 is strictly expressed in the stem cell compartment of white adipose tissue depots and completely absent in brown adipose tissue. Remarkably, p107-deficient stem cells uniformly give rise to brown-type adipocytes in vitro and in vivo. Furthermore, brown fat programming of mesenchymal stem cells by PRDM-BF1-RIZ1 homologous domain containing 16 (Prdm16) was associated with a dramatic reduction of p107 levels. Indeed, Prdm16 directly suppressed p107 transcription via promoter binding. Notably, the sustained expression of p107 blocked the ability of Prdm16 to induce brown fat genes. These findings demonstrate that p107 expression in stem cells commits cells to the white versus brown adipose lineage. STEM CELLS *2014;32:1323–1336*

INTRODUCTION

The ever-increasing prevalence of weight gain and obesity and their comorbidities of cardiovascular disease, type II diabetes, and cancers represent a significant health problem [1]. Obesity is a complex disease whereby environmental and genetic components collectively result in a positive energy balance. Functionally and morphologically different types of adipocytes play a crucial role in energy hemostasis by influencing glycemic and lipid control [2]. Different adipocyte lineages are localized within distinct anatomical regions throughout the body. In mammals, white adipocytes are distributed within major reservoirs located intra-abdominal (visceral) and in subcutaneous white adipose tissue (WAT) depots [3, 4]. Brown adipocytes that are found specifically between the scapulae in rodents and in the neck region of humans make up the classic brown adipose tissue (BAT) depot [4–6]. Another brown-type adipocyte, beige or brown in white (brite), is found dispersed within WAT depots where their development is enhanced by cold adaptation and β3 adrenergic stimulation [7–9]. In humans, beige adipocytes are found in the cervical, supraclavicular, axillary, and paravertebral anatomical locations [3]. Despite their nearly identical phenotypes, beige and brown adipocytes have different developmental origins [10, 11].

Brown-type adipocytes (both brown and beige) are mainly involved in metabolizing energy and heat production [12, 13]. In brown-type fat, oxidative phosphorylation is uncoupled such that the process of respiration is inefficient allowing for significant heat production (nonshivering thermogenesis) through consumption of calories without ATP synthesis. This process is facilitated by the upregulation of thermogenic promoting factors including uncoupling protein 1 (Ucp1) [12].

Studies demonstrate that brown-type adipocytes have antiobesity potential and can improve glycemic control. An original report estimated that as little as 50 g of BAT is sufficient to metabolize 20% of the daily energy needs of an individual if maximally stimulated [14]. In mice, genetic ablation of BAT causes a propensity toward obesity, diabetes, and hyperlipidemia [15, 16]. Moreover, increasing brown adipocyte activity using transgenic mice overexpressing Ucp1 produced a lean phenotype with reductions in fat stores and triglyceride levels [17, 18]. Whereas transplanted human or mouse brown adipocytes increased lipid and glucose tolerance and insulin sensitivity in mice [19, 20].

In humans, recent data suggest a role for brown-type adipocytes in metabolism since their amount was inversely correlated with body mass index (BMI) [21, 22]. This was

confirmed in a study that found activated brown-type adipocytes in most human subjects, except for the most obese [23]. The degree of activation correlated inversely with BMI and percentage of body fat, and directly with resting energy expenditure.

Thus, encouraging stem cells to differentiate into brown-type adipocytes would represent a novel approach to reduce positive energy balance and help combat metabolic diseases [24]. Evidence suggests that the three adipose lineages, white, brown, and beige, arise from committed progenitors known as preadipocytes. These were predominately derived from the lineage commitment of resident mesenchymal stem cells (MSCs), associated with the vasculature, of mesodermal and neuroectodermal origin [25–30]. MSCs and their precursors including the lineage committed preadipocytes are found within the stromal vascular fraction (SVF) of adipose tissue. Indeed, stem and progenitor cells within the SVF of human adipose tissue represent as much as 3% of the total number of cells [31]. Much of our current understanding of the transcriptional basis of adipocyte differentiation is based on studies using lineage committed cell lines [32]. However, very little is known regarding the transcriptional signals that commit MSCs to the white, brown, or beige lineages.

At the transcriptional level, the coregulator PRDM-BF1-RIZ1 homologous domain containing 16 (Prdm16) specifies the brown adipocyte fate [11, 33]. Expression of Prdm16 can stimulate a profound brown adipose selective gene expression pattern and in immortalized noncommitted murine embryonic fibroblasts (MEFs) forces a brown versus white adipose phenotype [33, 34]. Moreover, Prdm16 can act as a molecular switch determining the brown adipocyte over skeletal muscle lineage and determine the prothermogenic program of subcutaneous WAT in mice [11, 35].

The retinoblastoma susceptibility protein (Rb) family of transcriptional corepressors has also been implicated in adipocyte development. Much evidence suggests that the archetype family member Rb functions during adipogenesis and is involved in the maintenance of the terminal differentiated state [36–39]. p107, another Rb family member, has also been implicated in the development of adipose tissue. It is highly regulated during adipocyte differentiation of the committed preadipocyte cell line 3T3-L1 by increasing dramatically after day 1 and disappearing by day 7 [40, 41]. The importance of p107 to adipogenesis is highlighted by the inhibition of adipocyte differentiation during its knockdown in 3T3-L1 cells [42]. However, genetically deleted p107 (p107 KO) MEFs, which are an enriched source of noncommitted MSCs, can readily undergo adipocyte differentiation, with an increased potential over controls [37, 43]. Developmentally, p107 KO mice displayed a pronounced beige adipocyte phenotype with significant upregulation of Ucp1 suggesting that p107 regulates stem cell commitment to determine adipocyte lineage fates [44]. In this report, we now show that suppression of p107 expression in a stem cell autonomous manner is required for commitment of MSCs to the brown-type adipocyte fate. We found that suppression of p107 expression is required for commitment of MSCs to the brown-type adipocyte fate. Moreover, brown fat programming of MSCs by Prdm16 reduces p107 levels in stem cells; this reduction is required for the action of Prdm16 in brown fat. In summary, these findings demonstrate that p107 downregulation is necessary for lineage commitment of the brown over white adipocytes.

Materials and Methods

Mice and Dissections

All animal experiments were performed according to the guidelines approved by the Animal Care Committee of York University, Toronto, Canada. Experiments were performed on adult (8–16-week old) mice of the Balb/c genetic background, including those with a targeted deletion of p107 [44]. To stimulate brown type cell formation, some mice were injected at 1 mg/kg intraperitoneal, daily for 7 days with β3-adrenergic agonist, CL-316,243 (Sigma, St. Louis, MO, www.sigmaaldrich.com) diluted in saline. Various adipose depots were dissected for analysis.

Cell Types and Tissue Culture

MEFs representing an enriched source of primary MSCs were isolated from embryos of a heterozygous p107 KO mating pair at 14.5 days postcoitum. For isolation of the SVF, specific adipose depots were dissected, minced, and digested with 1 mg/ml collagenase I (Sigma) in Dulbecco's modified Eagle's medium (DMEM) supplemented with 10% fetal bovine serum (FBS) at 37°C for 45 minutes. After, the cell digested slurry was passed through a 100 μm cell strainer and cells were pelleted by centrifugation at 250*g* for 5 minutes and used immediately for analysis or cultured for adipogenic differentiation. C3H10T1/2 cells are a MSC line obtained from the American Type Culture Collection.

All cells were grown in DMEM 10% FBS and 1% penicillin/streptomycin. MEFs or C3H10T1/2 cells were differentiated to adipocytes after reaching confluence for 48 hours (time 0) as before [44]. The serum-free regimen for adipocyte differentiation used DMEM/F-12 (1:1) media instead of DMEM with 10% FBS. After 7 days of differentiation, some cultures were stained with oil red O for lipid.

Virus Production and Cell Line Derivation

For virus production of shp107 and control shRNA, the retroviral plasmids shp107 (TRCN0000218550; Sigma) and control pLKO.1 shRNA (TRCN0000218550; Sigma) were used. For Prdm16, pMSCV, and p107 virus production, the viral vectors pMSCV-PRDM16, pMSCV, and pBrit-p107 were used, respectively. C3H10T1/2 cells were transduced with 8 μg/ml of polybrene. After 24 hours cells were lysed or washed and refed for cell line derivation. Cell lines were derived by selecting virally transduced cells each with 2 μg/ml puromycin to produce MSC-shp107, MSC-shctl, MSC-Prdm16, MSC-Ctl, and MSC-p107.

Western Blot Analysis

For Western blot analysis, cells or tissue were lysed in RIPA buffer (0.5% Nonidet P40, 0.1% sodium deoxycholate, 150 mM NaCl, 50 mM Tris-Cl, pH 7.5) containing protease inhibitors (Roche, Mississauga, Canada, www.rochecanada.com/portal/ca). Protein lysates were Western blotted according to standard protocol. Antibodies used were anti-Ucp1 (Millipore, Billerica, MA, www.millipore.com), C18 anti-p107 (Santa Cruz, Biotechnology, Dallas, TX, www.scbt.com), rabbit polyclonal Prdm16, M-2 anti-Flag (Sigma), and monoclonal anti-α-tubulin (Sigma).

Transplantation

1×10^7 p107 KO MEFs, control Wt MEFs, or control Wt MEFs transduced with p107 were resuspended in 200 μl of saline, and transplanted subcutaneously into the sternum region of wild-type BALB/c mouse hosts. Brown adipocyte production was stimulated by CL-316,243 (Sigma) diluted in saline injected at 1 mg/kg intraperitoneal, daily for 7 days beginning on the day of the transplant. Six to eight weeks post-transplantation newly formed adipose tissue pads derived from the transplanted cells were excised and processed for histological analysis.

qPCR Analysis

For tissue culture RNA isolation, cells were lysed in RNA Lysis Buffer (FroggaBio, Toronto, Canada, www.froggabio.com) before RNA was purified using the Total RNA mini kit according to manufacturer's instructions (FroggaBio). For RNA isolation from adipose tissue, the TRIzol (Invitrogen, Carlsbad,CA, www.lifetechnologies.com) method was used according to the manufacturer's instruction. RNA (1 μg) was reverse transcribed into cDNA using the GeneAmp Kit (Applied Biosystems, Carlsbad, CA, www.lifetechnologies.com). Reverse transcribed RNA (25 ng) was used for PCR analysis. The qPCR assays were performed on the ABI 7500 Fast cycler using SYBR green PCR Master mix (Invitrogen). Primer sets (Supporting Information Table S1) and conditions for PCR were previously described elsewhere [45]. Relative expression of cDNAs was determined after normalization with β-actin using the $^{\Delta\Delta}$Ct method.

Microscopy

Images were obtained at room temperature using the Axiovert 40C (Carl Zeiss, Oberkochen, Germany, www.coporate.zeiss.com) microscope with ×10 0.25 LD A-Plan Ph1 Var1 or ×20 0.30 LD A-Plan Ph1 Var1 objectives. Digital images were captured using the Power Shot G5 camera with conversion lens adaptor LA-DC8B, 58–52 mm (Canon, Ota, Japan, www.canon.com) and were processed with Photoshop (Adobe, San Jose, CA, www.adobe.com).

Reporter Assays

C3H10T1/2 cells were transfected with increasing amounts of pMSCV-Prdm16 or pCMV E2F1, along with the 900 bp proximal p107 promoter fused to the luciferase gene (a kind gift from Dr. Julian Sage, Stanford University) [46]. pMSCV and pcDNA3 were used as "filler" controls. Transfection efficiency was normalized to renilla luciferase activity by addition of PRL-SV40. Twenty four hours post-transfection, luciferase activity was determined using the Dual-Luciferase assay kit (Promega, Madison, WI, www.promega.ca).

Quantitative Chromatin Immunoprecipitation Assay

Quantitative chromatin immunoprecipitation (qChIP) assay was performed on MSC-Prdm16 cells and the control cell line MSC-Ctl with an assay kit (Millipore) according to the manufacturer's instructions. E2F1 (Santa Cruz; sc-193) and Flag M2 (Sigma) antibodies were used for immunoprecipitation. ChIP primer sets (Supporting Information Table S1) amplified the promoters of p107 (−214 to −32) or positive control angiotensinogen (Agt) (−127 to +23). The PCR conditions were 40 cycles for 30 seconds at 95°C denaturation, 30 seconds at 56°C annealing, and 30 seconds at 72°C extension.

Competition Experiments

MSC-Prdm16 or MSC-p107 cells were untransduced (control) or transduced with p107 or Prdm16 retrovirus, respectively, all containing 8 μg/ml polybrene. After 24 hours, cells were washed and refed. Once confluent, 72 hours post-transduction, cells were differentiated and lysed after 7 days for qPCR analysis.

Measurement of Mitochondrial O_2 Respiration

Cells at 0, 3, and 7 days differentiation were first counted, resuspended in mitochondrial respiration media (MiRO5); 130 mM sucrose, 60 mM K-MES, 1 mM ethylene glycol tetraacetic acid, 3 mM $MgCl_2$, 10 mM K_2HPO_4, 20 mM HEPES, 1 mg/ml bovine serum albumin (pH 7.4), and permeabilized with 40 μg/ml saponin for 5 minutes at 37°C rotation. Saponin concentration was optimized by comparing the effect of a range of concentrations on State 3 respiration with exogenously added mitochondrial membrane intactness factor cytochrome c in all cell lines. After permeabilization, high resolution respirometry was conducted at 37°C with the Oroboros Oxygraph-2K (Innsbruck, Austria, www.oroboros.at) on 10^6 cells/chamber in MiRO5 buffer. For measurement of ADP-dependent oxidative phosphorylation (State 3 respiration) the following were added sequentially: (a) 5 mM glutamate + 2 mM malate (NADH generation for complex I-supported respiration), (b) 4 mM ADP, (c) 5 mM pyruvate (complex I substrate), and (d) 5 mM succinate ($FADH_2$ generation for complex II supported respiration). Two methods were used to assess mitochondrial O_2 consumption due to proton leak. First, measurements were made in the absence of ADP-stimulation of ATP synthase (State 2 respiration) with the addition of 5 mM glutamate and 2 mM malate to the permeabilized cells. Second, 10 μg/ml oligomycin was added after the addition of the complex 1 and II components of State 3 above.

Statistical Analysis

One-way ANOVA used a Tukey post hoc test. Student's paired *t* test was used unless otherwise stated. Results were considered to be statistically significant when $p < .05$.

Results

p107 Is Not Expressed in Terminally Differentiated Adipocytes and in BAT

To begin exploring the role for p107 in adipocyte lineage determination, we first examined p107 expression levels in adipose depots of adult mice relative to their epididymal pads. We found that p107 is expressed at high levels in visceral WAT (epididymal and retroperitoneal) (Fig. 1A). It is not expressed in interscapular BAT depots and is expressed at much lower levels in subcutaneous WAT, a depot known to contain more beige adipocytes (Fig. 1A) [35]. To determine whether p107 is differentially expressed in precursors or mature adipocytes, we fractionated adipose tissues into the terminally differentiated adipocytes and the SVF, containing MSCs and preadipocytes [29]. Interestingly, Western blot

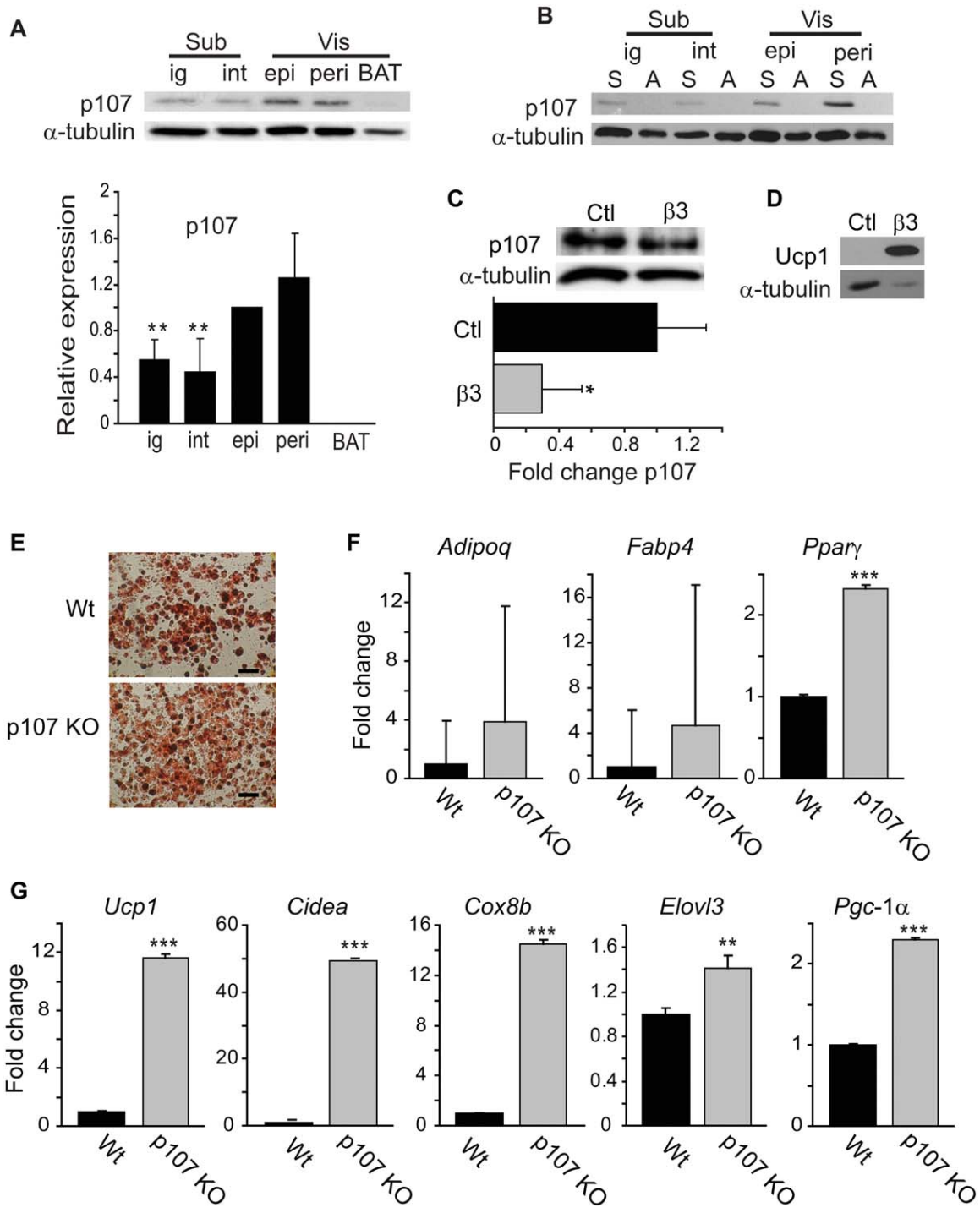

Figure 1. *p107* KO stromal vascular fraction (SVF) cells readily differentiate into brown-type adipocytes. **(A):** Representative Western blot and graphical representation for p107 protein levels of various subcutaneous (Sub) and visceral (Vis) adipose tissue depots of BALB/c mice relative to the epididymal testicular (epi) depot. Inguinal (ig), interscapular white adipose (int), and retroperitoneal (peri), and brown adipose tissue (BAT) ($n = 9$, one-way ANOVA $p < .01$, asterisks denote post-test significance $p < .01$). **(B):** Representative Western blot for p107 of the SVF (S) and the adipocyte fraction (A) of adipose pads from the subcutaneous and visceral depots of adult BALB/c mice. **(C):** Representative Western blot and graphical representation for p107 levels in the inguinal adipose depot of adult BALB/c mice treated with β3-adrenergic agonist, CL 316,243 (β3), or with vehicle saline control (Ctl) for 7 days. ($n = 6$; asterisk denotes significance $p < .05$). Values represent means ± SD. **(D):** Representative Western blot for Ucp1 of the inguinal adipose depot of adult BALB/c mice treated with β3-adrenergic agonist, CL 316,243 (β3), or with vehicle saline control (Ctl) for 7 days. **(E):** Representative oil red O staining of wild-type (Wt) and p107 KO SVF cells after 7 days of adipocyte differentiation (scale bar = 250 μm). **(F):** Gene expression analysis by qPCR for general adipogenic differentiation markers, *Adipoq*, *Fabp4*, and *Pparγ* ($p < .001$), in Wt and p107 KO SVF cells after 7 days of adipocyte differentiation ($n = 3$). **(G):** Gene expression analysis by qPCR for general brown-type adipocyte differentiation markers, *Ucp1* ($p < .001$), *Cidea* ($p < .001$), *Cox8b* ($p < .001$), *Elovl3* ($p < .01$), and *Pgc-1α* ($p < .001$), after 7 days of adipocyte differentiation of wild-type (Wt) and p107 KO SVF cells ($n = 3$, asterisks denote significance).

analysis revealed that p107 was uniquely expressed in the SVF and was undetectable in the mature adipocyte fraction of all depots (Fig. 1B). Moreover, p107 was significantly increased in the SVF of visceral compared to subcutaneous WAT. Thus, confirming that lower expression levels of p107 in resident stem cells within the subcutaneous adipose tissue of adult BALB/c mice are correlated with higher levels of beige adipocytes. Together, these results suggest that p107 functions in stem or progenitor cells to control the fate of differentiated adipocytes.

Treatment of animals with β-adrenergic activators is well known to increase the thermogenic program by increasing the number of beige adipocytes in subcutaneous WAT depots [28, 47]. We found that treatment of adult mice for 7 days with the synthetic β3-adrenergic agonist, CL-316,243, significantly ($p < .05$) reduced p107 protein levels in the subcutaneous (inguinal) adipose depot (Fig. 1C). This reduction coincided with the increased protein expression of the brown adipocyte marker Ucp1 in the subcutaneous (inguinal) adipose depot (Compare Fig. 1C with Fig. 1D). Thus, reduction of p107 expression in MSCs or their committed progenitors is correlated with increased beige adipocyte formation in vivo.

p107 KO Stem Cells Readily Differentiate into Brown-type Adipocytes In Vitro

We next tested whether p107 expression levels control adipocyte lineage commitment in a stem cell-autonomous manner. To accomplish this, we first assessed the SVF from the subcutaneous fat pads, which contain adult stem cells, for their capacity to control the fate of adipocyte differentiation. As had been published, oil red O staining 7 days postdifferentiation revealed that adipocyte differentiation was higher for the SVF of p107 KO over wild-type (Wt) mice [44] (Fig. 1E). Gene expression analysis of general adipogenic markers *Adipoq* and *Fabp4* showed no differences in levels, but *Ppar*γ levels were significantly increased in the differentiated SVF of p107 KO mice (Fig 1F). This increase might be reflective of the known enhanced adipocyte differentiation capacity of the p107 KO SVF [44]. The oxidative state of the differentiated cells was assessed by measuring the expression levels of various brown-type fat-selective genes (Fig. 1G). Convincingly, we found that adipocytes derived from p107 KO SVF had at least a sixfold ($p < .0001$) significantly higher gene expression level of the brown-type adipocyte marker *Ucp1* (Fig. 1G). The significantly higher expression levels of other brown-type markers, *Cidea*, *Cox8b*, *Elovl3*, and *Pgc-1*α, in differentiated p107 KO SVF corroborated the thermogenic character (Fig. 1G). These results suggest that p107 functions in stem and/or progenitor cells to block brown-type adipocyte differentiation.

p107 KO MEFs Readily Differentiate into Brown-type Adipocytes In Vitro

We confirmed that p107 expression levels control adipocyte lineage commitment within stem cells by assessing MEFs, an enriched source of primary MSCs. Both Wt and p107 KO MEFs underwent efficient conversion into adipocytes as observed by oil red O staining 7 days after induction of differentiation (Fig. 2A). Equivalent differentiation of Wt and p107 KO MEFs was confirmed by quantitative gene expression analysis for various general adipocyte markers, *Adipoq*, *Fabp4*, and *Ppar*γ (Fig. 2B). These results indicate that the deletion of p107 does not influence the ability of the cells to differentiate into adipocytes. However, after 7 days, we found that adipocytes derived from p107-deficient MEFs had at least a threefold ($p < .01$) higher mRNA level of the brown-type adipocyte marker *Ucp1* (Fig. 2C). We validated the brown-type adipocyte phenotype by assessing the gene expression levels of other brown-type versus white fat-selective markers, *Cidea*, *Cox8b*, *Elovl3*, and *Pgc-1*α, which were all significantly higher in p107-deficient cultures (Fig. 2D). However, gene expression levels for Ucp2, a homolog of Ucp1, were not affected (Fig. 2D). These results suggest that brown-type adipocyte differentiation is suppressed by p107 in primary stem cells.

p107 KO MEFs Readily Differentiate into Brown-type Adipocytes In Vivo

We examined whether p107 levels affect adipocyte fate during the in vivo differentiation of MSCs by transplanting p107 KO MEFs or control Wt MEFs alone or transduced with p107 into the sternum region of BALB/c mouse hosts. The formation of new adipose tissue pads can easily be discerned within 6–8 weeks postinjection of cells at this location, which has negligible endogenous adipose stores [33, 48, 49]. At 6 weeks post-transplantation, the newly formed adipose tissue, derived from transplanted cells, was excised for gene expression and histological analysis. Gross visualization of the tissue revealed that p107 KO MEFs readily produced multilocular appearing cells, which is a morphological hallmark of brown-type adipocytes (Fig. 2E) [4]. By contrast, Wt MEFs gave rise to unilocular appearing white adipocytes. The brown-type adipocyte formation of p107 KO MEFs was confirmed by gene expression analysis for *Ucp1*, which was significantly ($p < .05$) elevated in the ectopic tissue derived from p107 KO MEFs relative to Wt transplants (Fig. 2F). The sustained expression of p107 by viral transduction of the transplanted MEFs did not significantly alter the Ucp1 gene expression pattern in the newly formed tissue. These results establish that p107 controls the adipocyte lineage fate in culture and in vivo.

Knockdown of p107 in Stem Cells Stimulates Brown Fat Cell Differentiation

To avoid potential developmental effects caused by chronic loss of p107 in MEFs and to maintain a homogenous population of cells, we also used siRNA technology to knockdown p107 acutely in C3H10T1/2 MSCs. The C3H10T1/2 cell line has the potential to differentiate into different cell types including osteocytes and chondrocyte lineages, and they have been widely used to study brown and white adipocyte lineage potential [48, 50, 51]. We used retrovirus to deliver a short hairpin (sh) sequence for targeting p107 mRNA (shp107) or a nontargeting control (shctl) into C3H10T1/2 cells. Gene and protein expression analyses showed that p107 levels were significantly ($p < .01$) reduced by expression of shp107 (Fig. 3A). Consistent with our MEF studies, we found loss of p107 did not affect the adipogenic differentiation activity of C3H10T1/2 stem cells. Specifically, 7 days postdifferentiation, substantial lipid accumulation was visualized by staining with oil red O in both the MSC-shctl and MSC-shp107 cells (Fig. 3B). Adipocyte formation coincided with expression of general adipocyte markers *Adipoq*, *Fabp4*, and *Ppar*γ that were not significantly different between MSC-shctl and MSC-shp107 cells (Fig. 3C). However, there was a significantly higher protein expression

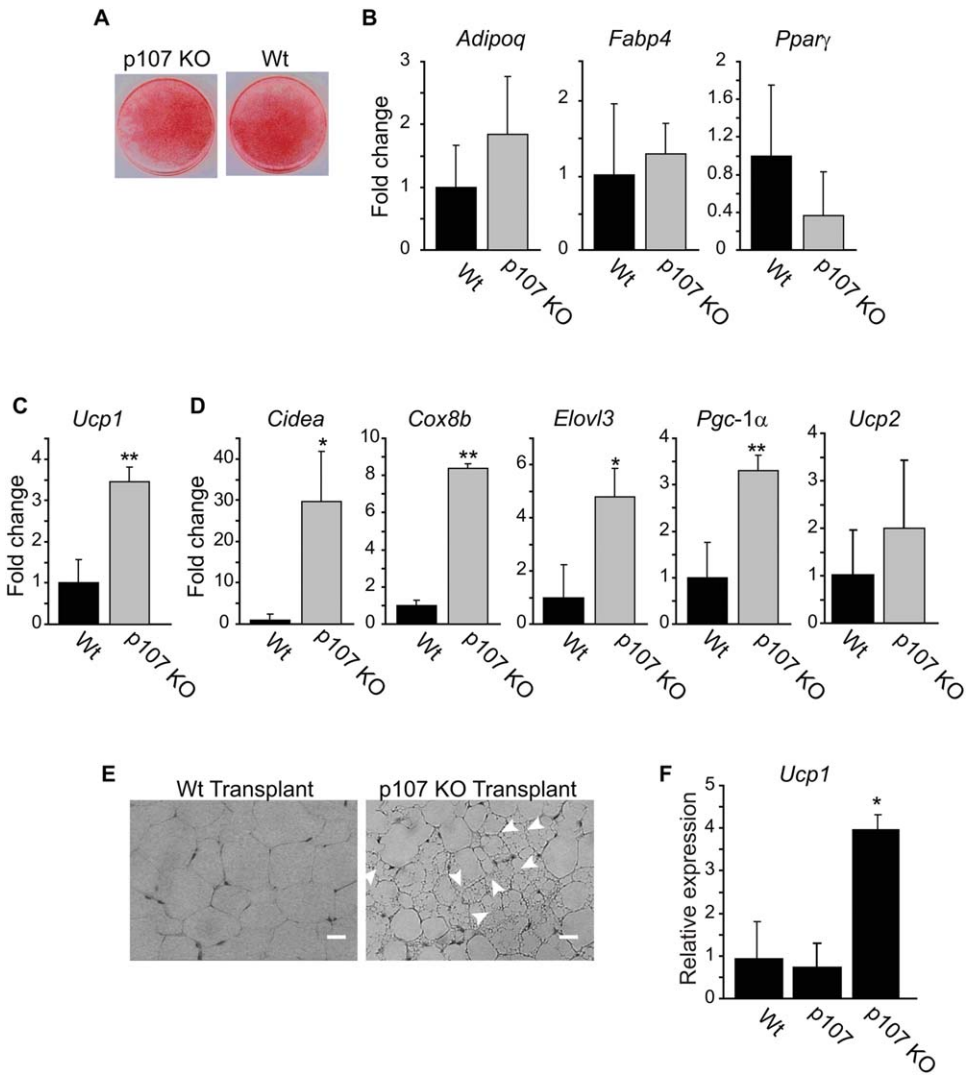

Figure 2. *p107* KO MEFs readily differentiate into brown-type adipocytes. **(A):** Oil red O staining for wild-type (Wt) control and p107 KO murine embryonic fibroblasts (MEFs) at 7 days postdifferentiation. **(B):** Gene expression analysis by qPCR for general adipogenic differentiation markers, *Adipoq*, *Fabp4*, and *Pparγ*, in Wt and p107 KO MEFs at 7 days postadipocyte differentiation ($n = 3$). **(C):** Gene expression analysis by qPCR of *Ucp1* in Wt and p107 KO MEFs at 7 days postdifferentiation ($n = 3$, asterisks denote significance, $p < .01$). **(D):** Gene expression analysis by qPCR for general brown-type adipocyte differentiation markers, *Cidea* ($p < .05$), *Cox8b* ($p < .01$), *Elovl3* ($p < .05$), *Pgc-1α* ($p < .01$), and *Ucp2* in Wt and p107 KO MEFs at 7 days postadipocyte differentiation ($n = 3$, asterisks denote significance). **(E):** Representative sections of tissue formation after 6 weeks of incubation with transplanted control wild-type Wt or p107 KO MEFs. Arrow heads denote the multilocular appearance of the tissue section indicative of the presence of brown adipocytes (scale bar = 50 μm). **(F):** Gene expression analysis by qPCR for *Ucp1* in tissue originating from subcutaneous transplants of donor Wt, Wt transduced with p107, and p107 KO MEFs relative to vehicle saline transplants ($n = 3$, asterisk denotes significance, $p < .05$). All the values represent means ± SD.

of Ucp1 over the course of 7 days of adipogenesis in p107-depleted MSCs (Fig. 3D). Strikingly, the p107-depleted cells expressed a near 400-fold more *Ucp1* mRNA compared to control cells at day 7 of differentiation (Fig. 3E). Importantly, the brown-type adipocyte phenotype was not limited to the expression of *Ucp1* since other brown lineage markers, including *Cidea*, *Elovl3*, and *Pgc-1α*, were also significantly increased in p107-depleted cells (Fig. 3E). As in the p107 KO MEFs, the gene expression levels for Ucp2 were not affected in the differentiated p107-depleted MSCs (Fig. 3E). Taken together, these results demonstrate that p107 functions in a stem cell autonomous manner to suppress the brown-type adipocyte fate.

p107 Knockdown Increases the Thermogenic and Oxidative Capacity of Differentiating Cells

To confirm that the thermogenic gene expression levels of the differentiated MSC-shp107 cells are reflected by a greater oxidative capacity, we assessed the O_2 consumption of the cells during adipocyte differentiation. High resolution respirometry revealed that during State 3 respiration, supported by both complex I and complex II substrates, the MSC-shp107 cells had significantly greater O_2 consumption than control cells in day 0, 3, or 7 days of differentiation (Fig. 4A). In addition, our results revealed a greater respiration due to proton leak

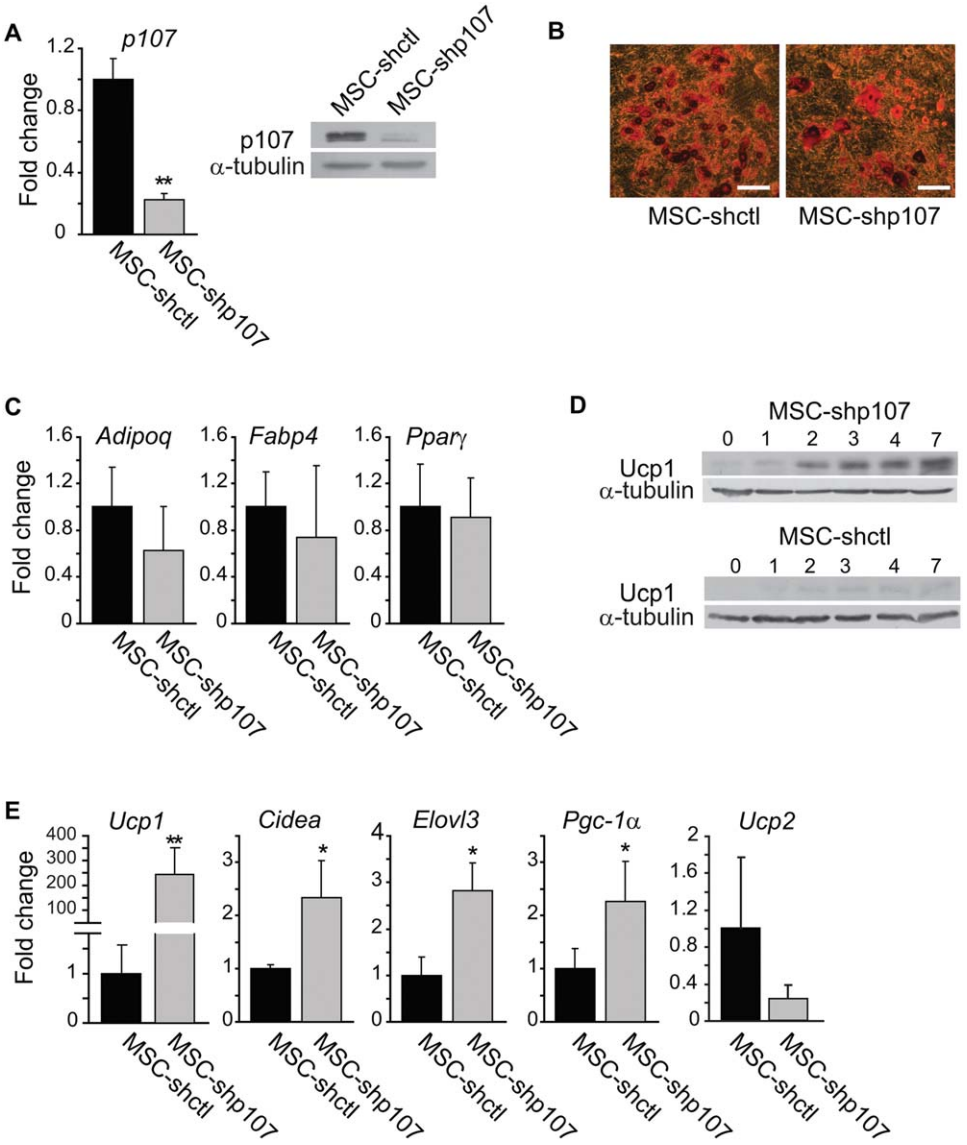

Figure 3. *p107* knockdown is required for brown-type adipocyte differentiation. **(A):** Gene expression and Western blot for p107 during growth in control MSC-shctl and MSC-shp107 cell lines ($n = 3$, asterisks denote significance $p < .01$). **(B):** Representative oil red O staining of control MSC-shctl and MSC-shp107 cell lines after 7 days of adipocyte differentiation (scale bar = 25 μm). **(C):** Gene expression analysis by qPCR for general adipogenic differentiation markers, *Adipoq*, *Fabp4*, and *Pparγ*, in control MSC-shctl and MSC-shp107 cell lines after 7 days of adipocyte differentiation ($n = 3$). **(D):** Representative Western blot for Ucp1 of control MSC-shctl and MSC-shp107 cell lines during a time course of adipocyte differentiation in days. **(E):** Gene expression analysis by qPCR for general brown-type adipocyte differentiation markers, *Ucp1* ($p < .01$), *Cidea* ($p < .05$), *Elovl3* ($p < .05$), *Pgc-1α* ($p < .05$), and *Ucp2*, after 7 days of adipocyte differentiation of control MSC-shctl and MSC-shp107 cell lines ($n = 3$, asterisks denote significance). Note the downregulation of p107 result in drastically elevated prothermogenic RNA. All values represent means ± SD.

when supported by substrates for complex I alone (GM) or both complex I and II (GMPS) with oligomycin for each of the days in differentiation (Fig 4B). Together, these data indicate that the oxidative and thermogenic capacities of the p107 depleted stem cells during differentiation are significantly enhanced.

p107 Knockdown in MSCs Influences Commitment Rather than Differentiation

As p107 is not expressed in terminally differentiated adipocytes (Fig. 1), it suggests that its reduction influences the lineage commitment of MSCs to brown-type adipocytes rather than their terminal differentiation. We tested for this possibility by assessing brown-type adipocyte formation when p107 levels were downregulated in control cells to the same levels as those in MSC-shp107 cells during differentiation. With normal serum conditions, p107 levels in MSC-shp107 cells are negligible by day 2 of differentiation compared to MSC-shctl control cells, and disappear for both cell types by day 7 (Fig. 5A). However, differentiation in serum-free media results in MSC-shctl cells with negligible p107 protein expression levels as in MSC-shp107 cells after 2 days (compare Fig. 5A with Fig. 5B). Although, the expression pattern for p107 was the same during differentiation, the MSC-shctl cells were unable to

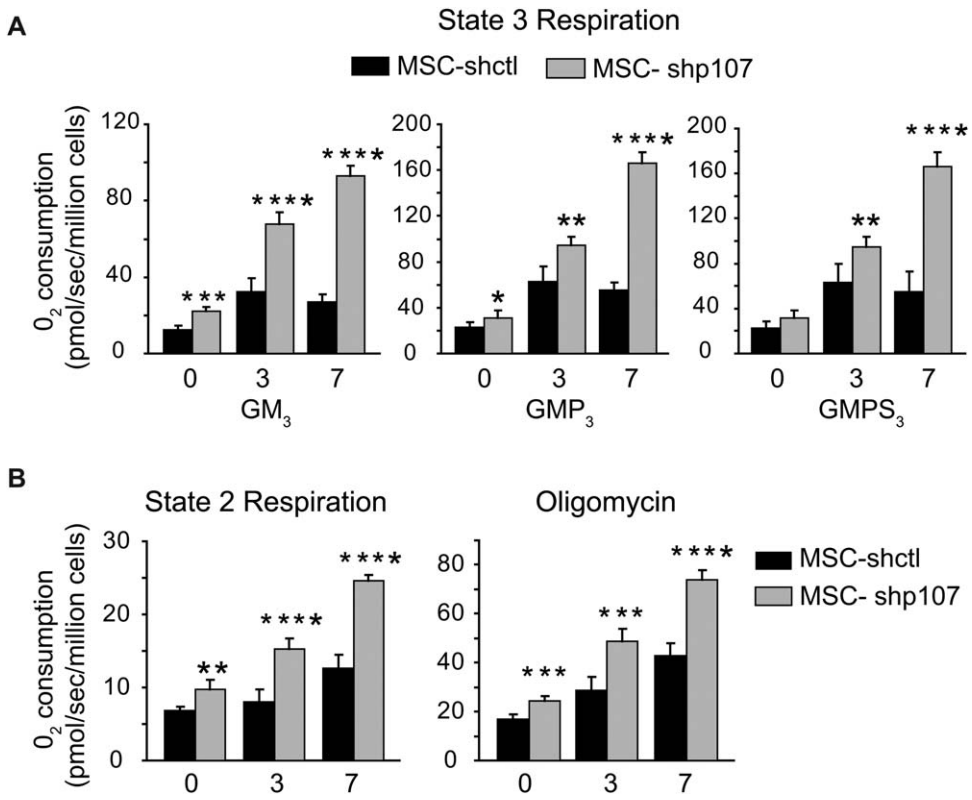

Figure 4. p107 depletion increases mitochondrial oxygen consumption during differentiation. **(A):** State 3 respiration reflecting the capacities for oxidative phosphorylation supported by both NADH-generating complex I substrates, glutamate and malate (GM_3) and pyruvate (GMP_3), and by $FADH_2$-generating complex II substrate succinate ($GMPS_3$) ($n = 5$, asterisks denote significance *, $p < .05$; **, $p < .01$; ***, $p < .001$; and ****, $p < .0001$). **(B):** Proton leak during State 2 respiration (non-ADP dependent respiration) assessed before the addition of ADP (complex I supported by GM_2) and in the presence of oligomycin after the addition of ADP (both complex I and II supported by $GMPS_3$) ($n = 5$, asterisks denote significance **, $p < .01$; ***, $p < .001$; and ****, $p < .0001$). All values represent means ± SD.

form brown-type adipocytes up to 7 days postdifferentiation as determined by the absence of Ucp1 (Fig. 5B). These results indicate that p107 expression must be downregulated at a time point prior to or at the very least immediately following brown-type adipocyte differentiation.

Prdm16 Downregulates p107 Expression

Prdm16 can drive the expression of a brown fat gene program in BAT and WAT [11, 33, 35]. Hence, we asked whether p107 plays a pivotal role in brown-type adipocyte lineage determination within the Prdm16 pathway. Indeed, the expression pattern for p107 is inversely proportional to Prdm16 in the subcutaneous WAT depots, with the difference increasing in response to treatment with probrowning, β3-adrenergic agonists (Fig. 1) [35].

To examine whether Prdm16 represses p107 expression or activity in MSCs, we created Flag-tagged Prdm16-expressing cell lines using retrovirus in CH310T1/2 cells. Prdm16-expressing cells readily express *Prdm16* RNA and protein as visualized by qPCR and Western blot, respectively (Fig. 6A). As anticipated, Prdm16-expressing MSCs differentiate into brown-type adipocytes expressing significant higher levels of *Ucp1*, as compared to control cultures (Fig. 6B) [34]. Interestingly, Western blot analysis showed that p107 protein levels were markedly reduced by Prdm16 expression in MSCs, prior to induction of differentiation (Fig. 6C). The effect of Prdm16 on p107 levels appeared to be transcriptional since *p107* mRNA levels were at least threefold lower in Prdm16-expressing relative to control MSCs. (Fig. 6D). By contrast, reducing p107 levels did not impact *Prdm16* mRNA (Fig. 6E) or protein (Fig. 6F) expression levels, in either the fibroblast stage or during a 7-day time course of adipogenic differentiation. Thus, Prdm16 reduces *p107* expression levels, but reductions in p107 levels do not affect *Prdm16* expression, suggesting that p107 is a downstream target of Prdm16 in the brown-type adipocyte lineage commitment pathway.

Prdm16 Downregulates p107 Gene Expression Directly

We next evaluated whether Prdm16 regulates p107 transcription. For this purpose, we used a construct containing 900 base pairs of the 5′ regulatory region and promoter proximal to the transcriptional start site of p107 fused to a luciferase reporter gene [46]. As previously shown, E2f1 expression significantly increased luciferase activity from this p107 construct (Fig. 6G). By contrast, increasing amounts of Prdm16 robustly suppressed p107 promoter activity (Fig. 6G), suggesting that Prdm16 might directly control p107 transcription.

Using qChIP assays, we assessed whether Prdm16 binds the promoter region of p107 (Fig. 6H). As C3H10T1/2 cells have negligible levels of Prdm16 (Fig. 6A), we used Flag-

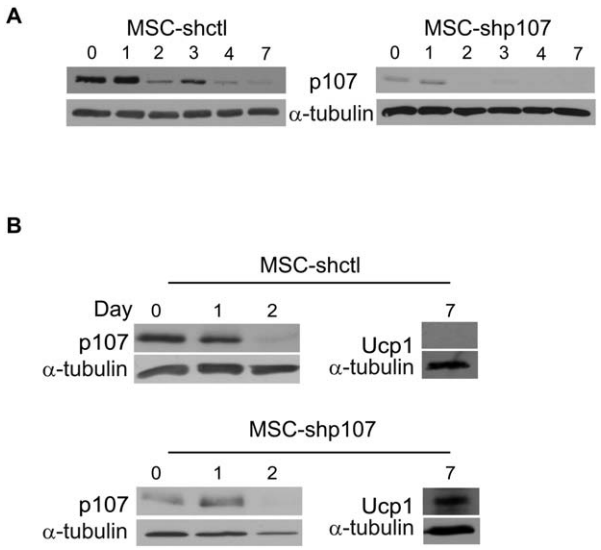

Figure 5. p107 knockdown in MSCs influences commitment rather than differentiation. **(A):** Representative Western blots for p107 MSC-shctl control and the MSC-shp107 cells during a time course of adipocyte differentiation in days using standard differentiation protocol. **(B):** Representative Western blots for p107 and UCP-1 on various days during a time course of adipocyte differentiation using serum-free media in the MSC-shctl control and the MSC-shp107 cells.

Prdm16-expressing or control vector-expressing MSC lines for binding assays. Prdm16-bound DNA regions were immunoprecipitated and purified using anti-Flag antibodies. Specific binding was evaluated by qPCR with primer sets within the 900 base pair (bp) promoter of p107 and to the positive control promoter, angiotensinogen (Agt) (Fig. 4H) [34]. As expected, E2f1 bound to p107 and not the Agt promoter sequences (Fig. 6H). Importantly, Prdm16 was enriched at both the positive control angiotensinogen (*Agt*) and *p107* promoters, but only in the cells engineered to express Flag-Prdm16 (Fig. 6H). Together, these data suggest that Prdm16 interacts with the p107 promoter region to downregulate p107 gene expression in precursor cells undergoing commitment to brown adipocytes.

p107 Blocks Prdm16 Function in Brown Fat Cell Commitment

Our experiments suggested that p107 is required for brown-type adipocyte development in MSCs. In order to assess the importance of p107 to the Prdm16 brown and beige adipocyte determination pathway, we performed "competition" assays. We first asked whether maintaining p107 expression could block the brown fat-inducing action of Prdm16. To accomplish this, MSC lines expressing Prdm16 were transduced with p107 retrovirus and subsequently differentiated (Fig. 7A). p107 over expression did not adversely influence adipocyte differentiation, as shown by staining lipids with oil red O (Fig. 7B). Note that the appearance of general adipogenic markers was at same levels in p107 treated and non-treated Prdm16 cell lines (Fig. 7C). Remarkably, *Ucp1* levels were significantly ($p < .05$) reduced by as much as sevenfold, during adipocyte differentiation (Fig. 7D). Other brown-type adipocyte markers *Cidea* and *Elovl3* were also significantly downregulated by p107 (Fig. 7D). Interestingly, the treatment had no effect on *Pgc-1α* gene expression levels. These results suggest that loss of p107 is necessary for Prdm16 to bring about the full brown-type adipocyte differentiation program.

Prdm16 Cannot Rescue Brown-type Adipocyte Differentiation in the Presence of p107

The importance of p107 in the Prdm16 brown-type adipocyte-forming pathway was further corroborated by evaluating the phenotype of p107-overexpressing cell lines (MSC-p107), transduced with Prdm16 retrovirus (Fig. 7E). Oil red O and general adipogenic factor expression showed that MSC-p107 overexpressing cell lines differentiated equivalently whether or not they also expressed Prdm16 (Fig. 7F, 7G). However, the excessive Prdm16 levels were unable to increase Ucp1 expression in MSC-p107 cultures, even after 7 days of differentiation (Fig. 7H). Expression levels of other brown adipocyte markers *Cidea* and *Elovl3* were similarly unaffected by Prdm16 (Fig. 7H). Intriguingly, the gene expression levels of *Pgc-1α* were rescued by Prdm16. This unequivocally demonstrates that p107 is a necessary downstream target of Prdm16, required to promote the full brown-type (brown and beige) adipocyte differentiation program in adult cells.

Discussion

In this study, we found that p107 controls adipocyte lineage fate decisions of white versus brown-type (beige and brown) adipocytes in a stem cell autonomous manner. We demonstrated that both genetic and shRNA-mediated reduction of p107 in MSCs resulted in a prothermogenic differentiation program in vitro and in vivo. Our results add to the premise that p107 is an important nodal point during stem cell fate decisions. To date, there is evidence that it controls the lineage specification of different neuronal and skeletal muscle cell types during differentiation [45, 52].

The complete absence of p107 within interscapular BAT depots further supports the notion that it is a crucial component for adipocyte lineage fate decisions. A hypothesis confirmed by the conspicuous scarcity of white adipocytes in BAT. The deficiency of p107 in BAT precursors might relate to the different stem cell types and progenitors involved with tissue development compared to WAT [10, 11]. However, tonic levels of sympathetic outflow to BAT may also actively suppress p107 expression [12]. It would be of interest to assess whether p107 expression increases in BAT in response to denervation or thermo neutral conditioning of animals.

Increased Prdm16 expression and beige adipocyte formation in subcutaneous depots corresponds to the significantly lower p107 levels in the stem cell fraction of adult subcutaneous fat that was reduced further with β-adrenergic treatment. Indeed, we provide evidence that Prdm16 targets the downregulation of p107 expression directly to cause commitment to the brown-type adipocyte lineage. Although Prdm16 must downregulate p107 in MSCs for brown fat determination, specifically depleting p107 in MSCs to produce brown-type adipocytes does not require an increase in Prdm16 expression. This observation suggests that reduction of p107 is a major target gene for Prdm16 in lineage commitment, which is able to execute much of the downstream program. It hints at the possibility that other

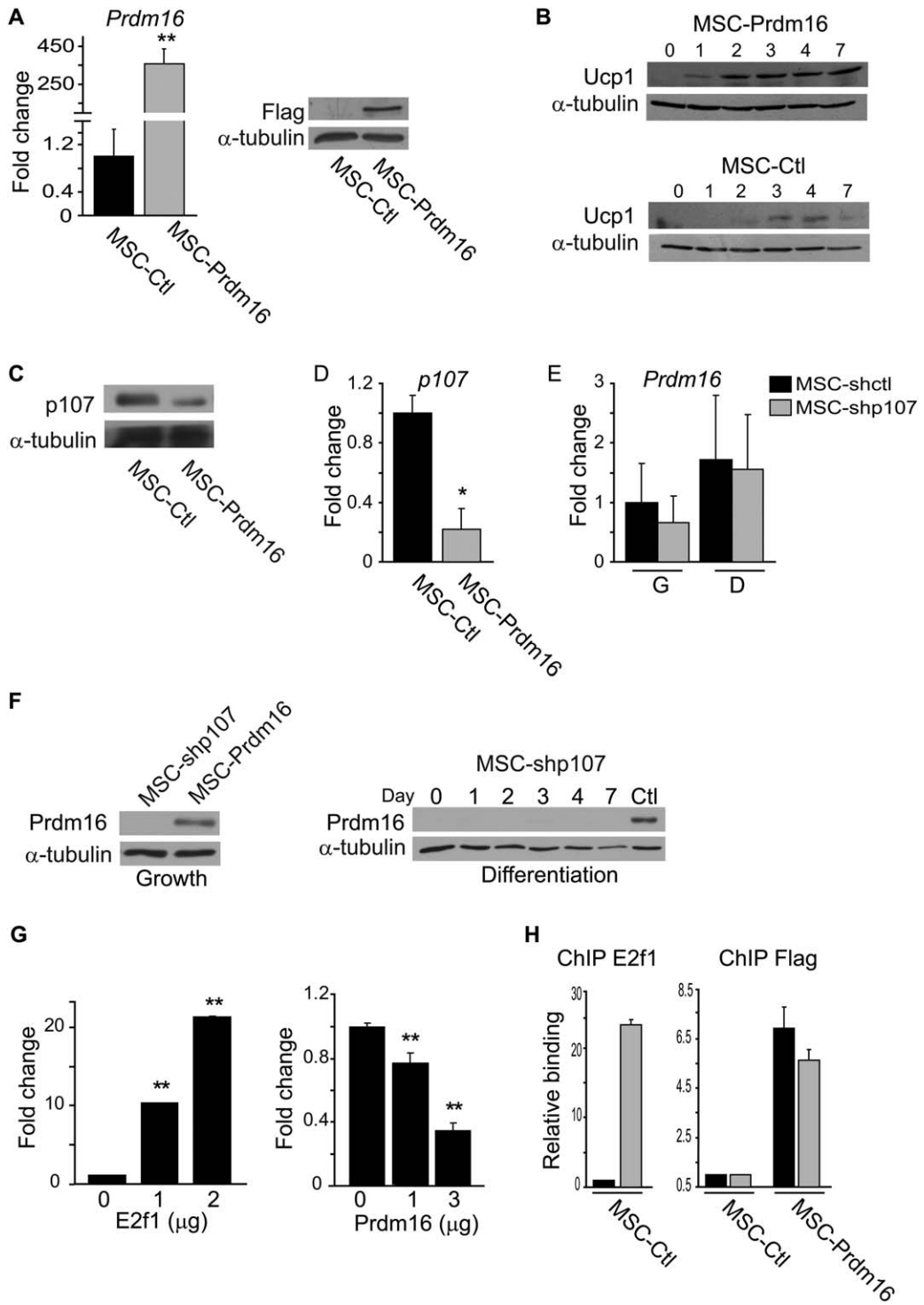

Figure 6. Prdm16 regulates the gene expression of *p107*. **(A):** Gene expression analysis by qPCR for *Prdm16* and representative protein levels by Western blot for Flag-tagged Prdm16 in MSC-Ctl and MSC-Prdm16 cell lines ($n = 3$, asterisk denotes significance, $p < .01$). **(B):** Representative Western blot for Ucp1 of MSC-Ctl and MSC-Prdm16 cell lines during a time course (days) of adipocyte differentiation. **(C):** Representative Western blot of p107 in the MSC-Ctl and MSC-Prdm16 cell lines. **(D):** Gene expression analysis by qPCR for *p107* in different MSC-Ctl and MSC-Prdm16 cell lines ($n = 3$, asterisk denotes significance, $p < .05$). Note that p107 RNA and protein levels are reduced in the Prdm16 overexpressing stem cell lines. **(E):** Gene expression analysis by qPCR for *Prdm16* in different MSC-shctl and MSC-shp107 cell lines during growth (G) and after 7 days in adipocyte differentiation (D) ($n = 3$). **(F):** Representative Western blot for Prdm16 protein in the MSC-shctl and MSC-shp107 cell lines during growth and adipocyte differentiation. Note that *Prdm16* RNA and protein are not expressed in the MSC-shp107 cell line suggesting that p107 is downstream of Prdm16 function. **(G):** Fold change in luciferase activity using the 900 bp proximal *p107* promoter transfected with increasing amounts of E2f1 or Prdm16 in C3H10T1/2 cells. For E2f1, $n = 3$ one-way ANOVA $p < .0001$, asterisks denote post-test significance $p < .01$ and for Prdm16 $n = 7$, one-way ANOVA $p < .0001$, asterisks denote post-test significance $p < .01$). **(H):** Quantitative ChIP analysis for Flag-tagged Prdm16 in different MSC-Ctl and MSC-Prdm16 cells, and for E2f1 in MSC-Prdm16 cells amplifying with primers for the mouse promoters of p107 (-214 to -32, gray bars) or positive control Agt (-127 to $+23$, black bars) ($n = 3$). All values represent means $\pm$ SD. Abbreviations: ChIP, chromatin immunoprecipitation.

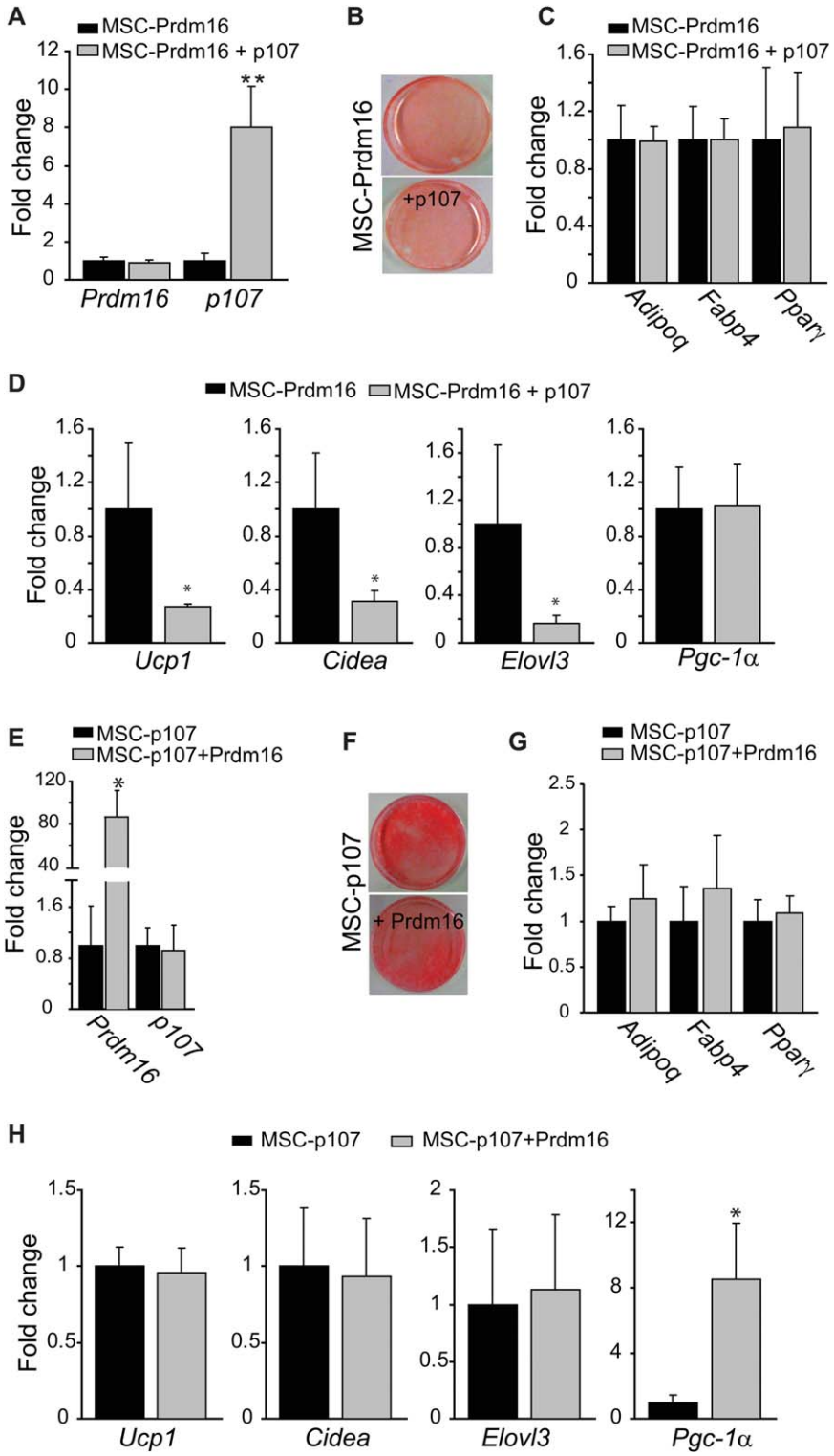

Figure 7. p107 overrides Prdm16 function in brown fat cell commitment. **(A):** *Prdm16* and *p107* mRNA expression in MSC-Prdm16 and MSC-Prdm16 cells transduced with p107 retro virus after 7 days of adipocyte differentiation (asterisks denote significance, for $n = 3$, $p < .01$). **(B):** Representative oil red O staining of MSC-Prdm16 and MSC-Prdm16 cells transduced with p107 retro virus after 7 days of adipocyte differentiation. **(C):** Gene expression analysis by qPCR for general adipogenic differentiation markers, *Adipoq*, *Fabp4*, and *Pparγ*, in MSC-Prdm16 and MSC-Prdm16 cells transduced with p107 retro virus after 7 days of adipocyte differentiation ($n = 3$). **(D):** Gene expression analysis by qPCR for general brown-type adipocyte differentiation markers *Ucp1*, ($n = 4$, $p < .05$), *Cidea* ($n = 3$, $p < .05$), *Elovl3* ($n = 3$, $p < .05$), and P*gc-1α* ($n = 3$), after 7 days of adipocyte differentiation in MSC-Prdm16 and MSC-Prdm16 cells transduced with p107 retro virus (asterisks denote significance). Note that p107 blocks brown-type differentiation capacity despite the presence of Prdm16. **(E):** *Prdm16* and *p107* mRNA expression in MSC-p107 and MSC-p107 cells transduced with Prdm16 retro virus after 7 days of differentiation ($n = 3$, asterisk denotes significance $p < .05$). **(F):** Representative oil red O staining of MSC-p107 and MSC-p107 cells transduced with Prdm16 retro virus after 7 days of adipocyte differentiation. **(G):** Gene expression analysis by qPCR for general adipogenic differentiation markers, *Adipoq*, *Fabp4*, and *Pparγ*, in MSC-p107 and MSC-p107 cells transduced with Prdm16 retro virus after 7 days of adipocyte differentiation ($n = 3$). **(H):** Gene expression analysis by qPCR for general brown-type adipocyte differentiation markers, *Ucp1*, *Cidea*, *Elovl3*, and *Pgc-1α*, after 7 days of adipocyte differentiation in MSC-p107 and MSC-p107 cells transduced with Prdm16 retro virus ($n = 3$, asterisk denote significance, $p < .05$). Note that Prdm16 cannot rescue brown-type differentiation. All values represent means ± SD.

browning agents or adaptations such as Irisin, Fgf21, and exercise might function via reduction of p107 [53–55].

p107 might be a crucial factor that receives external metabolic signals to accordingly adjust how stem cells will react and differentiate to maintain adipocyte homeostasis. Currently, the metabolic cues that direct the upstream signaling pathways for lineage specification through p107 are not known. For example, studies have shown that white adipocyte hyperplasia by recruitment and differentiation of stem cells occurs during high fat feeding and in the obesogenic state [56–58]. Hence, the increase in white adipocyte numbers might be associated with the sustained expression levels of p107, nonetheless the signaling pathway(s) that is activated is not clear. Conversely, the ligand BMP7 has been shown to commit stem cells to the brown-type lineage potentially through the Smad signaling pathway which ultimately relays its signal to Smad 4 [48, 59]. As a potential upstream signaling pathway, it is noteworthy that p107 in complex with E2f4 has been shown to associate with Smad 3 and Smad 4 to interact on the c-myc promoter [60].

It is not clear how p107 functions during lineage commitment of adipocytes. p107 is a transcriptional corepressor that does not bind to DNA directly but through transcription factors, most notably E2f4 [61]. The levels of p107/E2f4 complexes increase the length of time in the G1 phase of the cell cycle by repressing the promoters of genes involved in the G1 to S phase transition. The G1 phase of the cell cycle is an important opportunity for cells to become influenced by extracellular signals, to develop new signaling pathways, and undergo substantive chromatin modifications [62, 63]. One scenario for how p107 might influence stem cell fates is based on the length of time the uncommitted stem cell remains in G1. Time spent at this stage might be a crucial factor for cell fate changes to occur. According to this hypothesis, factors involved in white adipocyte commitment would require a greater length of time in G1 to bring about their lineage-specific effects. In contrast, if the uncommitted stem cells received adipocyte differentiation signals in the absence of p107, their length of time within G1 is significantly reduced such that the white adipocyte fate would not be possible and only brown-type cells would develop instead.

Recently, Rb has been shown to be important in establishing fate choice between bone and brown adipocytes in vivo [64]. However, unlike p107, Rb functions during adipogenesis and for the maintenance of the terminally differentiated state rather than commitment of stem cells. In accordance with this idea is the finding that simian virus 40 (SV40) antigen that inactivates Rb results in the inhibition of adipogenesis in committed white preadipocyte cells [65]. In addition, Rb-deficient fibroblasts are unable to differentiate into white adipocytes [37, 66]. Contrarily, p107 KO primary SVF cells and MEFs readily differentiate into adipocytes [37, 44]. Furthermore, in difference to p107, Rb is expressed in both terminally differentiated brown and white adipocytes in vivo and in vitro [36, 38]. In this capacity, Rb might provide a means to control adipocyte homeostasis and energy expenditure by sensing metabolic signals that impact on its gene expression and/or phosphorylation status. For example, in brown adipocytes, Rb undergoes phosphorylation upon the cold-induced upregulation of Ucp1 [38]. In addition, for terminally differentiated white adipocytes, the conditional deletion of Rb produces a brown-type adipocyte phenotype [39]. Consistent with this are transgenic mice overexpressing SV40 antigen specifically in terminally differentiated adipocytes that transformed white fat into brown-type adipocytes and continuously activated Ucp1 in interscapular BAT [67].

Conclusions

Studying the intrinsic changes in the expression levels of p107 and its subsequent effect on thermoregulation is critical. This is highlighted during physiological insults, such as traumatic burns or lipodegeneration, where stem cell activation and commitment might ultimately be regulated by p107 function. Moreover, understanding the underlying mechanisms of stem cell commitment to the different adipocyte lineages can lead to effective treatment strategies for the ongoing metabolic problems that plague society. The identification of the role of p107 in specifying the adipose lineages at the level of the stem cell raises the possibility that it might be amenable for therapeutic manipulation for the treatment of type II diabetes and obesity.

Acknowledgment

We thank Dr. Guillaume Grenier for critical insights and careful reading of the manuscript.

Author Contributions

M.D. and D.P.P.: performed experiments, designed experiments and analyzed the data, created unique materials, discussed the results, and commented on the manuscript; A.S.: Performed experiments, designed experiments and analyzed the data, created unique materials, discussed the results, commented on the manuscript, conceived and developed the hypothesis, led the project, interpreted the data, and wrote the manuscript; C.G.R.P.: designed experiments and analyzed the data, discussed the results, and commented on the manuscript; P.S.: created unique materials, discussed the results, and commented on the manuscript.

Disclosure of Potential Conflicts of Interest

The authors indicate no potential conflicts of interest.

References

1 Ahima RS. Digging deeper into obesity. J Clin Invest 2011;121:2076–2079.

2 Bartelt A, Heeren J. The holy grail of metabolic disease: Brown adipose tissue. Curr Opin Lipidol 2012;23:190–195.

3 Gesta S, Tseng YH, Kahn CR. Developmental origin of fat: Tracking obesity to its source. Cell 2007;131:242–256.

4 Cinti S. The adipose organ. Prostaglandins Leukot Essent Fatty Acids 2005;73:9–15.

5 Cypess AM, White AP, Vernochet C et al. Anatomical localization, gene expression profiling and functional characterization of adult human neck brown fat. Nat Med 2013;19:635–639.

6 Lidell ME, Betz MJ, Leinhard OD et al. Evidence for two types of brown adipose tissue in humans. Nat Med 2013;19:631–634.

7 Ghorbani M, Himms-Hagen J. Appearance of brown adipocytes in white adipose tissue during CL 316,243-induced reversal of obesity and diabetes in Zucker fa/fa rats. Int J Obes Relat Metab Disord 1997;21:465–475.

8 Himms-Hagen J, Melnyk A, Zingaretti MC et al. Multilocular fat cells in WAT of CL-316243-treated rats derive directly from

white adipocytes. Am J Physiol Cell Physiol 2000;279:C670–681.
9 Xue B, Coulter A, Rim JS et al. Transcriptional synergy and the regulation of Ucp1 during brown adipocyte induction in white fat depots. Mol Cell Biol 2005;25:8311–8322.
10 Timmons JA, Wennmalm K, Larsson O et al. Myogenic gene expression signature establishes that brown and white adipocytes originate from distinct cell lineages. Proc Natl Acad Sci USA 2007;104:4401–4406.
11 Seale P, Bjork B, Yang W et al. PRDM16 controls a brown fat/skeletal muscle switch. Nature 2008;454:961–967.
12 Cannon B, Nedergaard J. Brown adipose tissue: Function and physiological significance. Physiol Rev 2004;84:277–359.
13 Bartelt A, Bruns OT, Reimer R et al. Brown adipose tissue activity controls triglyceride clearance. Nat Med 2011;17:200–205.
14 Rothwell NJ, Stock MJ. Luxuskonsumption, diet-induced thermogenesis and brown fat: The case in favour. Clin Sci (Lond) 1983; 64:19–23.
15 Lowell BB, S-Susulic V, Hamann A et al. Development of obesity in transgenic mice after genetic ablation of brown adipose tissue. Nature 1993;366:740–742.
16 Feldmann HM, Golozoubova V, Cannon B et al. UCP1 ablation induces obesity and abolishes diet-induced thermogenesis in mice exempt from thermal stress by living at thermoneutrality. Cell Metab 2009;9:203–209.
17 Kopecky J, Clarke G, Enerback S et al. Expression of the mitochondrial uncoupling protein gene from the aP2 gene promoter prevents genetic obesity. J Clin Invest 1995; 96:2914–2923.
18 Rossmeisl M, Kovar J, Syrovy I et al. Triglyceride-lowering effect of respiratory uncoupling in white adipose tissue. Obes Res 2005;13:835–844.
19 Nishio M, Yoneshiro T, Nakahara M et al. Production of functional classical brown adipocytes from human pluripotent stem cells using specific hemopoietin cocktail without gene transfer. Cell Metab 2012;16:394–406.
20 Stanford KI, Middelbeek RJ, Townsend KL et al. Brown adipose tissue regulates glucose homeostasis and insulin sensitivity. J Clin Invest 2013;123:215–223.
21 Cypess AM, Lehman S, Williams G et al. Identification and importance of brown adipose tissue in adult humans. N Engl J Med 2009;360:1509–1517.
22 Saito M, Okamatsu-Ogura Y, Matsushita M et al. High incidence of metabolically active brown adipose tissue in healthy adult humans: Effects of cold exposure and adiposity. Diabetes 2009;58:1526–1531.
23 van Marken Lichtenbelt WD, Vanhommerig JW, Smulders NM et al. Cold-activated brown adipose tissue in healthy men. N Engl J Med 2009;360:1500–1508.
24 Tseng YH, Cypess AM, Kahn CR. Cellular bioenergetics as a target for obesity therapy. Nat Rev Drug Discov 2010;9:465–482.
25 Tran KV, Gealekman O, Frontini A et al. The vascular endothelium of the adipose tissue gives rise to both white and brown fat cells. Cell Metab 2012;15:222–229.
26 Gupta RK, Mepani RJ, Kleiner S et al. Zfp423 expression identifies committed preadipocytes and localizes to adipose endothelial and perivascular cells. Cell Metab 2012;15:230–239.
27 Tang W, Zeve D, Suh JM et al. White fat progenitor cells reside in the adipose vasculature. Science 2008;322:583–586.
28 Lee YH, Petkova AP, Mottillo EP et al. In vivo identification of bipotential adipocyte progenitors recruited by beta3-adrenoceptor activation and high-fat feeding. Cell Metab 2012;15:480–491.
29 Cawthorn WP, Scheller EL, MacDougald OA. Adipose tissue stem cells meet preadipocyte commitment: Going back to the future. J Lipid Res 2012;53:227–246.
30 Billon N, Dani C. Developmental origins of the adipocyte lineage: New insights from genetics and genomics studies. Stem Cell Rev 2012;8:55–66.
31 Fraser JK, Zhu M, Wulur I et al. Adipose-derived stem cells. Methods Mol Biol 2008; 449:59–67.
32 Farmer SR. Transcriptional control of adipocyte formation. Cell Metab 2006;4:263–273.
33 Seale P, Kajimura S, Yang W et al. Transcriptional control of brown fat determination by PRDM16. Cell Metab 2007;6:38–54.
34 Kajimura S, Seale P, Tomaru T et al. Regulation of the brown and white fat gene programs through a PRDM16/CtBP transcriptional complex. Genes Dev 2008;22:1397–1409.
35 Seale P, Conroe HM, Estall J et al. Prdm16 determines the thermogenic program of subcutaneous white adipose tissue in mice. J Clin Invest 2011;121:96–105.
36 Puigserver P, Ribot J, Serra F et al. Involvement of the retinoblastoma protein in brown and white adipocyte cell differentiation: Functional and physical association with the adipogenic transcription factor C/EBPalpha. Eur J Cell Biol 1998;77:117–123.
37 .Classon M, Kennedy BK, Mulloy R et al. Opposing roles of pRB and p107 in adipocyte differentiation. Proc Natl Acad Sci USA 2000; 97:10826–10831.
38 .Hansen JB, Jorgensen C, Petersen RK et al. Retinoblastoma protein functions as a molecular switch determining white versus brown adipocyte differentiation. Proc Natl Acad Sci USA 2004;101:4112–4117.
39 Dali-Youcef N, Mataki C, Coste A et al. Adipose tissue-specific inactivation of the retinoblastoma protein protects against diabesity because of increased energy expenditure. Proc Natl Acad Sci USA 2007; 104:10703–10708.
40 Richon VM, Lyle RE, McGehee RE, Jr. Regulation and expression of retinoblastoma proteins p107 and p130 during 3T3-L1 adipocyte differentiation. J Biol Chem 1997;272: 10117–10124.
41 Timchenko NA, Wilde M, Iakova P et al. E2F/p107 and E2F/p130 complexes are regulated by C/EBPalpha in 3T3-L1 adipocytes. Nucleic Acids Res 1999;27:3621–3630.
42 May JS, Prince AM, Lyle RE et al. Antisense suppression of p107 inhibits 3T3-L1 adipocyte differentiation. Biochem Biophys Res Commun 2001;283:837–842.
43 Landsberg RL, Sero JE, Danielian PS et al. The role of E2F4 in adipogenesis is independent of its cell cycle regulatory activity. Proc Natl Acad Sci USA 2003;100:2456–2461.
44 Scime A, Grenier G, Huh MS et al. Rb and p107 regulate preadipocyte differentiation into white versus brown fat through repression of PGC-1alpha. Cell Metab 2005;2: 283–295.
45 Scime A, Soleimani VD, Bentzinger CF et al. Oxidative status of muscle is determined by p107 regulation of PGC-1α. J Cell Biol 2010;190:651–662.
46 Burkhart DL, Wirt SE, Zmoos AF et al. Tandem E2F binding sites in the promoter of the p107 cell cycle regulator control p107 expression and its cellular functions. PLoS Genet 2010;6:e1001003.
47 Granneman JG, Li P, Zhu Z et al. Metabolic and cellular plasticity in white adipose tissue I: Effects of beta3-adrenergic receptor activation. Am J Physiol Endocrinol Metab 2005;289:E608–616.
48 Tseng YH, Kokkotou E, Schulz TJ et al. New role of bone morphogenetic protein 7 in brown adipogenesis and energy expenditure. Nature 2008;454:1000–1004.
49 Tran TT, Kahn CR. Transplantation of adipose tissue and stem cells: Role in metabolism and disease. Nat Rev Endocrinol 2010;6:195–213.
50 Tang QQ, Otto TC, Lane MD. Commitment of C3H10T1/2 pluripotent stem cells to the adipocyte lineage. Proc Natl Acad Sci USA 2004;101:9607–9611.
51 Tang QQ, Lane MD. Adipogenesis: From stem cell to adipocyte. Annu Rev Biochem 2012;81:715–736.
52 Vanderluit JL, Wylie CA, McClellan KA et al. The Retinoblastoma family member p107 regulates the rate of progenitor commitment to a neuronal fate. J Cell Biol 2007;178:129–139.
53 Bostrom P, Wu J, Jedrychowski MP et al. A PGC1-alpha-dependent myokine that drives brown-fat-like development of white fat and thermogenesis. Nature 2012;481:463–468.
54 Fisher FM, Kleiner S, Douris N et al. FGF21 regulates PGC-1alpha and browning of white adipose tissues in adaptive thermogenesis. Genes Dev 2012;26:271–281.
55 De Matteis R, Lucertini F, Guescini M et al. Exercise as a new physiological stimulus for brown adipose tissue activity. Nutr Metab Cardiovasc Dis 2013;23:582–590.
56 Maumus M, Sengenes C, Decaunes P et al. Evidence of in situ proliferation of adult adipose tissue-derived progenitor cells: Influence of fat mass microenvironment and growth. J Clin Endocrinol Metab 2008;93:4098–4106.
57 Joe AW, Yi L, Even Y et al. Depot-specific differences in adipogenic progenitor abundance and proliferative response to high-fat diet. Stem Cells 2009;27:2563–2570.
58 Roldan M, Macias-Gonzalez M, Garcia R et al. Obesity short-circuits stemness gene network in human adipose multipotent stem cells. FASEB J 2011;25:4111–4126.
59 Sellayah D, Bharaj P, Sikder D. Orexin is required for brown adipose tissue development, differentiation, and function. Cell Metab 2011;14:478–490.
60 Chen CR, Kang Y, Siegel PM et al. E2F4/5 and p107 as Smad cofactors linking the TGFbeta receptor to c-myc repression. Cell 2002;110:19–32.
61 Wirt SE, Sage J. p107 in the public eye: An Rb understudy and more. Cell Div 2010;5:9.
62 Orford KW, Scadden DT. Deconstructing stem cell self-renewal: Genetic insights into

cell-cycle regulation. Nat Rev Genet 2008;9:115–128.

63 Lange C, Calegari F. Cdks and cyclins link G1 length and differentiation of embryonic, neural and hematopoietic stem cells. Cell Cycle 2010;9:1893–1900.

64 Calo E, Quintero-Estades JA, Danielian PS et al. Rb regulates fate choice and lineage commitment in vivo. Nature 2010;466:1110–1114.

65 Higgins C, Chatterjee S, Cherington V. The block of adipocyte differentiation by a C-terminally truncated, but not by full-length, simian virus 40 large tumor antigen is dependent on an intact retinoblastoma susceptibility protein family binding domain. J Virol 1996;70:745–752.

66 Hansen JB, Petersen RK, Larsen BM et al. Activation of peroxisome proliferator-activated receptor gamma bypasses the function of the retinoblastoma protein in adipocyte differentiation. J Biol Chem 1999;274:2386–2393.

67 Ross SR, Choy L, Graves RA et al. Hibernoma formation in transgenic mice and isolation of a brown adipocyte cell line expressing the uncoupling protein gene. Proc Natl Acad Sci USA 1992;89:7561–7565.

See www.StemCells.com for supporting information available online.